

ELECTROMAGNETOHYDRODYNAMIC MIXED CONVECTION FLUID FLOW BETWEEN TWO PARALLEL PLATES

الحمل المختلط لسريان الموائع بين سطحين متوازيين خلال مجال كهرومغناطيسي

A.M. El-Zahaby^a, M. K. Bassiouny^b, A. Khalil^a, E.A. El-Shenawy^a, E. A. El-Agouz^a and M. I. Amro^a

a- Mechanical power engineering dept., Faculty of engineering, Tanta University, Egypt

b- Mechanical power engineering dept., Faculty of engineering, Menofia University, Egypt

ملخص البحث:

- تم عمل موديل عددي لسريان الموائع الموصلة للتيار الكهربى - ماء مالح- (بنسبة كتله 25% كلوريد الصوديوم) تحت تأثير المجالات الكهربيه و المغناطيسيه باستخدام ديناميكا الموائع الحسايبه. حيث تم استخدام طريقه الأحجام المتناهيه الصغر فى حل معادله نافير- استوك فى وجود القوى الكهرومغناطيسيه (قوى لورنس). بالإضافة إلى معادله الطاقة مع الأخذ فى الاعتبار تأثير كلا من الطاقة المتبدده نتيجة تأثير جول و تأثير اللزوجه. تم تطبيق معادله التدويم و داله السريان لتجزئه معادلات الموديل. وقد تم حل المعادلات باستخدام طريقه الحذف لجاوس. و تم الحصول على القوى الكهرومغناطيسيه المؤثرة على السريان باستخدام معادله ماكسويل و قانون أوم.

- تم كتابة برنامج فورتران يعمل على حل المعادلات الجبريه غير الخطيه للموديل، حيث تم الحصول على توزيع السرعة للسريان ثنائى الاتجاه لأرقام هارتمان مختلفه و رقم رينولد ثابت، كما تم الحصول على توزيع السرعات أيضاً لأرقام رينولد مختلفه عند ثبات رقم هارتمان.

تم استنتاج تأثير معامل التيار الكهربى الخارجى فى توزيع السرعات و درجات الحرارة، كما تم استنتاج تأثيره على سرعة السريان. تم تحليل و مقارنة توزيع السرعات و درجات الحرارة لحالات كثيره تحت تأثير معامل التيار الكهربى الخارجى و بدونه.

تم اختيار الموديل لمدى كبير من أرقام هارتمان، و كيرشوف، بالإضافة إلى معامل التيار الكهربى الخارجى و فى حدود رقم رينولد من 50 إلى 2000. الموديل صالح لأى قيمه لرقمى براندتل و إيكيرت و يسمح بدراسة معاملات التشغيل و خواص سريان الحرارة مع الأخذ فى الاعتبار الطاقة المتبدده نتيجة لتأثير جول و تأثير اللزوجه.

تم التحقق من صحة الموديل العددي المستخدم فى الحل عن طريق مقارنة نتائجه بنتائج معملية فى البحث و أخرى تحليلية و حسايبه عن آخرين و التى أعطت إتفاقا بينها.

ABSTRACT

A numerical model of the flow of electrically conducting fluid -salt water- (pure water+25% by weight NaCl) under the influence of an imposed electric and magnetic fields is analyzed using computational fluid dynamic techniques. A finite volume method is used to solve the Navier-stokes equations with the effect of Lorentz force and energy equations for the fluid variables. The Vorticity stream function formulation is applied to discrete the model equations. The algebraic equations are solved by using the Gauss-elimination method. The Lorentz force is obtained by solving the Maxwell's equation and ohm's law via the same finite volume technique. The model equations are solving using a self written FORTRAN CODE, which solve the nonlinear algebraic equations. Velocity profiles for a two dimensional flow are predicted for a different Hartmann's numbers at a constant Reynolds's number, also at a different Reynolds's numbers at a constant Hartmann's number.

E. A. El-Agouz and M.I. Amro

The effect of External Electrical current parameter E_f in accelerating or decelerating the flow is predicted. The velocity distribution and temperature contours were computed for many cases under the effect of E_f . The different ranges for the effects of the E_f were analyzing and discussed.

The model is valid for a laminar flow ($Re= 50: 2000$) with a wide range of the effected parameters H_a , Gr , and E_f . The calculations are valid for any values for Pr , Ec .

The model allows studying the effect of operating parameters on fluid flow and heat transfer characteristics taking into account the effect of Joule and viscous dissipating energy effect.

The model is validated by comparing its results with experimental results by PIV laser system, analytical results, and with the theoretical results obtained by Dennis and Dulikravich,2000 [1] and other authors. The comparison shows good agreement.

NOMENCLATURES

B, B_0	applied magnetic field intensity , tesla
C_p	specific heat, kJ/kg.K
D_h	hydraulic diameter, m
E	electric field strength Volt/m
Ec	Eckert Number
E_f	external electric field factor
g	gravity acceleration, m/s^2
Gr	Grashof number
h	Convection heat transfer coefficient, $W/m^2.K$
H	channel height , m
H_a	Hartmann number
J	electric current density , A/m^2
k	thermal conductivity, $W/m.K$
l, L	dimensional, dimensionless length, m , (-)
L_f	Lorentz force, N
Nu	local Nusselt number
P	pressure, Pa
Pr	Prandtl number
Q	heat input, Joule
q'''	heat source power per unit volume W/m^3
Re	Reynolds's number
T	temperature, K
U_o, V	dimensionless horizontal and vertical velocities
u, v	dimensional horizontal and vertical velocities m/s
x, y, z	dimensional coordinates, m
X, Y, Z	Dimensionless coordinates

Greek symbols	
ν	kinematic viscosity m^2/s
θ	dimensionless temperature
ρ	Density, kg/m^3
ψ	Dimensionless stream function
ω	Dimensionless Vorticity
σ	Electrical conductivity, $1/Ohm. m$
α	thermal diffusivity of the fluid m^2/s
ϕ	General variable
β	coefficient of volumetric thermal expansion of the fluid, $1/K$
Subscripts	
f	fluid
m	mean
tot	total
Abbreviations	
CCD	Charge coupled device
DNS	direct numerical simulation
EHD	electrohydrodynamics
EMFD	electromagnetofluidynamics
EMHD	electromagnetohydrodynamics
FVM	finite volume method
MHD	magnetohydrodynamics
ND-	Neodym diode
RMS	root mean squire
PIV	particle image velocimetry
YAG	(yttrium –aluminum – garnet)

1. Introduction

The study of fluids flow containing electric charges under the influence of an externally applied electric field and negligible magnetic field is known as electrohydrodynamics or EHD. The study of fluids flow influenced only by an externally magnetic field is known as

magnetohydrodynamics or MHD. While the study of fluids flow under the combined influence of the externally applied electric and magnetic fields often called Electromagnetohydrodynamics EMHD or Electromagnetofluidynamics EMFD.

E. A. El-Agouz and M.I. Amro

Formally, EMHD deals with the combined effects of electrically conducting fluids and electromagnetic forces, and has been an area of research since the late 1930s.

EMHD addresses all phenomena related to the interaction of electric and magnetic fields with electrically conducting fluids. When an electrically conducting fluid moves through a magnetic field, it produces an electric field and subsequently an electric current. The interaction between the electric current and electromagnetic fields creates a body force, called the Lorentz force, which acts on the fluid itself. In this case the phenomenon is known as magnetohydrodynamics MHD, but if the Lorentz force is created due to an external electric and magnetic field, it is known as Electromagnetohydrodynamics EMHD.

The Lorentz force tends to suppress turbulence to a certain extent and modify the flow field. EMHD flow control provides a prospective method that could be used in many industrial applications, ranging from power generation, propulsion system to hypersonic vehicles and atmospheric reentry vehicles, Setsuo Takezawa et al, 1995 [2].

Numerical simulations of many important processes such as the growth of single crystals, metal casting for aerospace applications, aluminum electrolysis, require sophisticated tools for coupled

fluid flow- heat/mass transfer – electromagnetic fields. In summary, computational EMHD is vital subject of recent research with a long list of interdisciplinary applications and scientific problems.

In the last years, a growing interest has been addressed to the study of EMHD effects on mixed and natural convective flows, such interest in the topic is due to the large number of possible technological applications, like in metallurgy, where the quality of the materials, produced in regime of controlled crystal growth, can be influenced by the effect of an external electromagnetic fields. Recently being increased the efforts towards the realization of nuclear fusion machines. Effects of an EMHD in liquid metal flows are studied to design properly critical components, e.g. blankets of reactors, such studies could be found in Sidorenkov et al, (1995), [3], Kumamamaru et al, (2004) [4], Mao et al, (2008), [5], Sharma and Singh, (2009), [6] and Vetcha et al, (2009), [7].

For the natural convection problem solution, Aslan, 2010, [8] developed and investigated a 2D nonlinear incompressible magnetohydrodynamics code to solve the steady 2D natural convection problems. The developed code can be accurately used for the solutions of MHD equations.

The heat transfer by mixed convection with the effect of electromagnetic fields was investigated in many studies, e.g. Saleh and Hashim, 2010 [9], Umavathi et al, 2011, [10], where the fully developed mixed MHD convection in vertical channels was investigated. They studied and presented graphically the effect of various parameters such as Hartmann's number, aspect ratio and buoyancy parameter with considering the effect of viscous dissipation and Joule heating.

A direct numerical simulation (DNS) code was done by O'Sullivan and Biringen, 1997 [11] and developed by Schuster and Luo, 2009, [12]. They used hybrid Fourier pseudo spectral-finite difference discretization scheme and fractional step technique, to simulate a 2D MHD channel flow.

The system is described by the MHD equations which are a combination of the Navier Stokes equations and the magnetic induction equation, which is derived from the Maxwell equations. The laminarization effect of the imposed magnetic field is studied and the heat transfer is incorporated into the code in order to assess the effect of control on the heat transfer properties.

The steady laminar flow of electrically conducting incompressible fluid between two parallel plates of a channel in the presence of magnetic field was

investigated by Ganesh and Krishnambal, 2006 [13] and the solution for the case of small Reynolds number and Hartmann's number is discussed. Expressions for velocity components and the pressure were obtained. The governing nonlinear equations were solved numerically and the graphs of axial and radial velocity profiles had been drawn.

In horizontal channels, the effect of magnetohydrodynamics in mixed convection was investigated by Linga and Murty, 2011 [14]. They investigated the MHD heat transfer in fully developed viscous flow of an ionized gas taking into account different geometrical considerations. Rahman et al, 2011, [15], investigated the effect of magnetohydrodynamic in mixed convection in a horizontal channel with an open cavity. They obtained the numerical solutions for a wide range of Rayleigh, Reynolds and Hartmann numbers. The average Nusselt number at the heated surface, the drag force and the mean temperature of the fluid in the cavity are calculated.

The present work is a 2D numerical and experimental investigation of EMHD mixed convection heat transfer in horizontal channel. The objective of the present work is to quantify the effects of the ratio between the height and width of the channel. Also, the effect of operating

E. A. El-Agouz and M.I. Amro

dimensionless parameters as Re, Ht, Gr, Ec, Pr and external electric field factor Ef on the fluid flow and heat transfer characteristics are presented.

2. Experimental Work

Particle Image Velocimetry PIV is a well-established technique for the measurements of instantaneous planar velocity fields and has been reviewed by a number of authors as Raffel et al., 1998 [16]. In its simplest form, the flow is illuminated with a double pulsed light sheet and the positions of tracer particles are recorded with a CCD camera viewing normal to the plane of the sheet. The main displacement vector of the particle images within each small region, divided by the laser pulse separation time, gives the local flow velocity vector. In the present work, the images taken by the camera were processed with PIV cross-correlation technique using interrogation area of 32x32 Pixels. Measurements are performed using a model of a Perspex rectangular channel; the used cross section has 60 mm height, 120mm width and 300mm length. The laser sheet has two measuring planes one is horizontal to measure the side plane velocity and the other is vertical plane which is the main plane for flow which is compared with the numerically calculated velocity field. The test section, electromagnet device, positive/negative electrodes, camera and laser source are

shown in Fig. (1). The layout of the used test rig and measuring system is shown in Fig. (2).

A double pulse ND: YAG laser was used to set-up the light sheet. The output energy is 30 mJ (for each pulse) at 532 nm with pulse duration of 6ns. The essential element for the generation of the light sheet is a cylindrical lens. Combinations of lenses were used to generate thin light sheets of high intensity. The adjustment of the light sheet thickness was done by adjusting the separation between the two spherical lenses. The PIV velocity measurements reported here are the ensemble means of 20 realizations since averaged values (mean and RMS) show good convergence for at least 20 cycles. Twenty instantaneous velocity fields were measured at each cross section and different conditions. The velocity fields were investigated at different operating conditions. The ensemble-mean velocity at each point on the grid, $\langle \bar{V}(x, y) \rangle$, is then computed as the mean of the instantaneous velocity values at each grid point, or $\langle \bar{V}(x, y) \rangle = \left[\frac{1}{N} \right] \sum_{i=1}^{N=20} \bar{V}_i(x, y)$ Where $\bar{V}_i(x, y)$ is the instantaneous velocity at the (x, y) grid node in the i th realization and N is the total number of realization ($N=20$ in the present work). Where, $\langle u \rangle$, $\langle v \rangle$ are the two components of $\langle \bar{V}(x, y) \rangle$ in the vertical cross-section measurement plane.

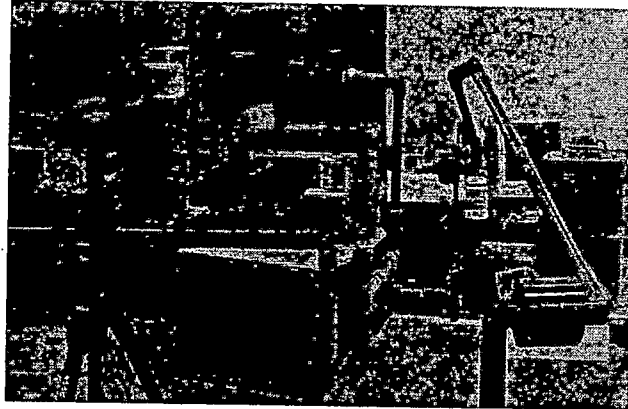


Fig.1 Particle Image Velocimetry (PIV) and tested cross section.

- 1-Moneter
- 2-AC/DC Electric current bridge
- 3- Condenser
- 4- Input current key
- 5- Variac I
- 6- Variac II
- 7- Laser sheet
- 8- Centrifugal pump
- 9-Delivery pipe
- 10- Electromagnet
- 11- U tube
- 12- Orifice meter
- 13- Storage tank
- 14- Honey comp
- 15- CCD camera
- 16- Laser arm
- 17- Power supply
- 18- Laser tube
- 19- PIV CPU system
- 20- Key board

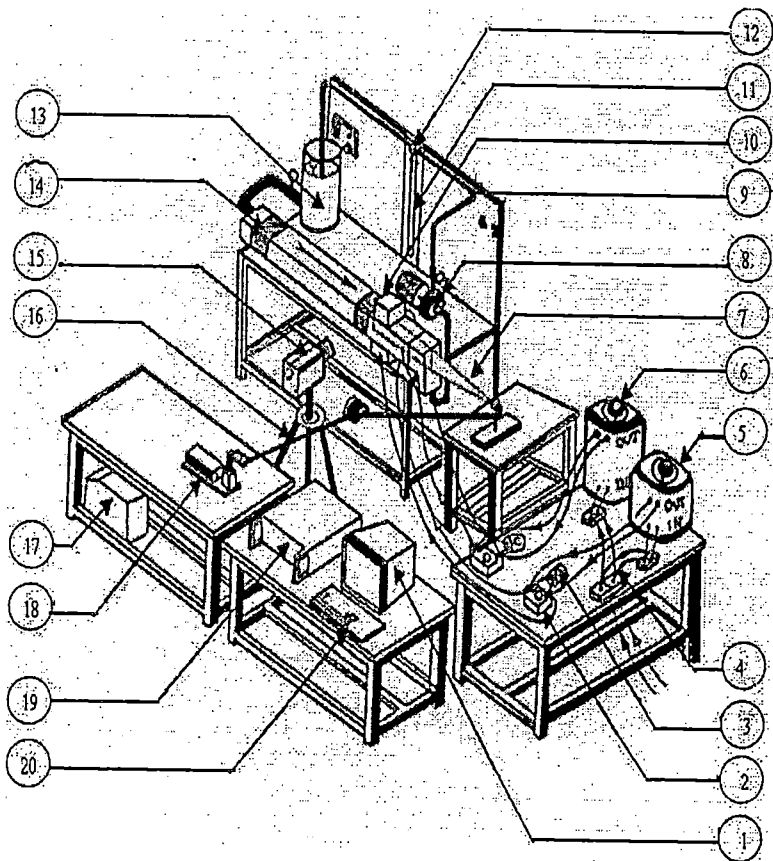


Fig.2 Layout of the experimental test rig and visualization system (PIV)

E. A. El-Agouz and M.I. Amro

3. MATHEMATICAL MODELING

The Electromagnetohydrodynamics EMHD mixed convection flow through two-dimensional channel is assumed to be represented by a steady, viscous, incompressible, and laminar. The effect of thermal radiation is not considered. The considered governing equations are the continuity, momentum and energy equations. Constant thermo-physical properties are assumed.

As shown in this Fig. (3), two parallel plates are extending in X and Z directions, the electrically conducting fluid flows in the X direction, the constant transverse magnetic field is imposed in the Z-direction and a constant DC external

electric field applied orthogonally on the direction of flow and magnetic field.

3.1 Statement of the problem

The schematic of the coordinate system and the corresponding physical configuration are shown in fig. (3). External water enters the channel with uniform velocity U_0 and constant temperature T_0 and leaves the channel carrying the heat dissipated due to the temperature difference between the inlet temperature and the walls temperature, also due to the heat dissipated due to the Joule heating and viscous dissipating energy.

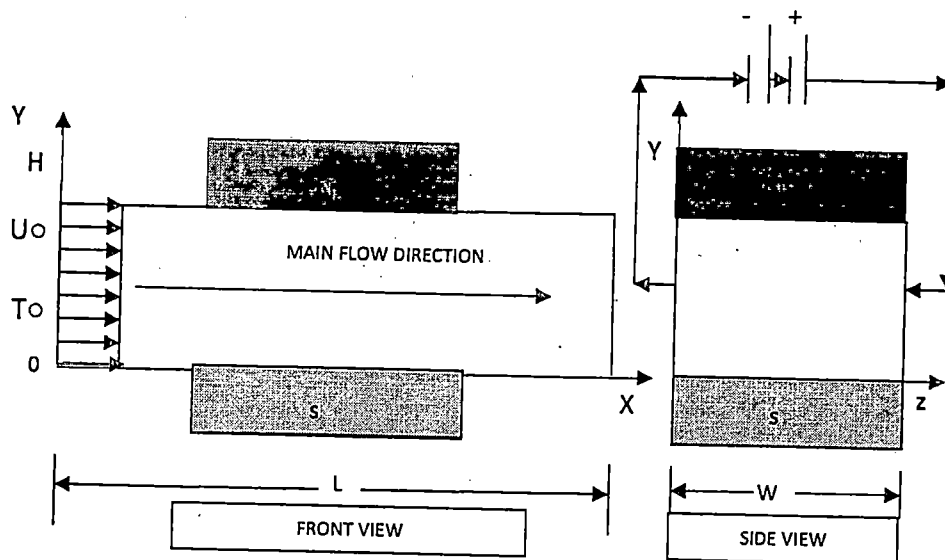


Fig.3 Physical configuration and coordinates system

3.2 Full Set of EMHD Equations:

The considered simplifying assumptions are steady, two dimensional, laminar,

incompressible, and fully developed Hartmann flow and the physical properties of the fluid are independent of the temperature and constant. The fully

3.5 Boundary Conditions:

The dimensionless of the initial and boundary conditions are given as:

At the channel inlet:

$$X = 0 \text{ and } 0 \leq Y \leq 1 \text{ and } T = T_0, U = 1, V = 0, \theta = 0$$

At the wall surfaces

$$\frac{\partial \theta}{\partial X} = 0, U = V = 0 \text{ (Insulated)}$$

At the channel exit section U, V and θ are extrapolated.

4. Numerical solution:

A finite volume method FVM, procedure discussed by Patanker, 1980, [19] and Versteeg and Malalasekera, 1995, [20] has been used for discretizing the governing equations. The computational domain in two dimensions has been discretised using control volumes of uniform size. Convection-diffusion terms have been treated by the central differencing scheme. The governing equations are integrated over the control volume with the use of linear interpolation inside the finite element, and the obtained algebraic equations are solved by the Gauss-Seidel method. The above mentioned numerical method has been implemented in a self-written FORTRAN computer code which, solve non-linear partial differential equations in two dimensions. The domain is subdivided into

a number of control volumes each associated with a grid point. The governing equations are integrated over control volume, shown in Fig. 4, the following general form for the diffusion-convection equation, (13) is used to solve the model equations:

$$\frac{\partial}{\partial X}(\Phi U) + \frac{\partial}{\partial Y}(\Phi V) = \frac{\partial}{\partial x} \left(\Gamma \frac{\partial \Phi}{\partial X} \right) + \frac{\partial}{\partial Y} \left(\Gamma \frac{\partial \Phi}{\partial Y} \right) + (S_u + S_p, \Phi) \quad (13)$$

The two terms in the left-hand side of equation (13), are the convection terms, while the first term and second terms of the right-hand side represent the diffusion terms, the third is the source term.

In figure 4 the points P, E, W, N and S denote the points with the coordinates

(i,j) , $(i+1,j)$, $(i-1,j)$, $(i,j+1)$, and $(i,j-1)$ respectively.

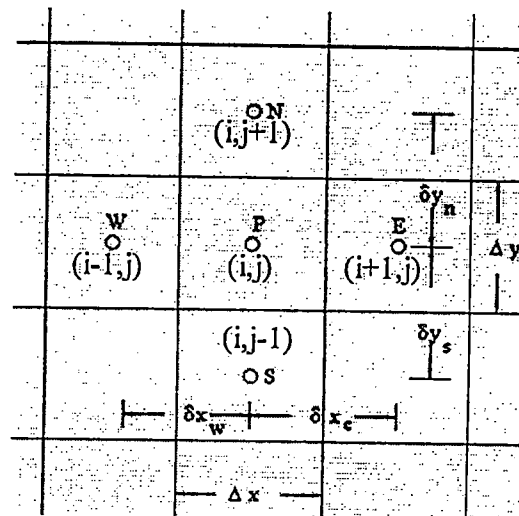


Fig. 4 Grid system for the computational domain

In equation (13), central difference for the diffusion terms and upwind difference for the convection terms are used, then, general form of algebraic equation is given as:

$$\Phi_P = \left(\begin{matrix} a_E \Phi_E + a_W \Phi_W \\ + a_N \Phi_N + a_S \Phi_S + b \end{matrix} \right) / a_P \quad (14)$$

where a_P, a_E, a_W, a_N, a_S and "b" are the coefficients of the equivalent algebraic equations.

4.1 Vorticity Equation ω :

Applying then previous technique on the momentum equation (10), the algebraic form of the Vorticity can be given as follows:

$$\omega_P = \left(\begin{matrix} a_E \omega_E + a_W \omega_W \\ + a_N \omega_N + a_S \omega_S + b \end{matrix} \right) / a_P \quad (15)$$

4.2 Stream Equation ψ :

Applying previous technique for the stream equation (13), the algebraic form of the stream function, ψ , has the following form:

$$\psi_P = (a_E \psi_E + a_W \psi_W + a_N \psi_N + a_S \psi_S) / a_P \quad (16)$$

4.3 Velocity Components U and V:

In order to get the values of the velocity components in the X and Y direction, applying previous technique on the Eq.10, the algebraic form of the U and V can be given as follows:

$$U_P = \frac{\psi_N - \psi_S}{2 \Delta Y} \quad (17)$$

$$V_P = \frac{\psi_W - \psi_E}{2 \Delta X} \quad (18)$$

4.4 Temperature Equation θ :

Finally, applying previous technique on the dimensionless energy Eq.(6), the algebraic form of dimensionless temperatures, θ_P , can be given as follows:

$$\theta_P = (a_E \theta_E + a_W \theta_W + a_N \theta_N + a_S \theta_S) / a_P \quad (19)$$

The obtained algebraic equations of the Vorticity, stream function, temperature, and velocity components are solved using the Gauss-eliminating method. An iterative solution procedure is employed to obtain the steady state solution of the considered problem. The convergence criteria used for all field variables ($\varphi = \psi, \omega, \theta$) for every point is:

$$\varepsilon = \frac{\sum_{j=1}^{j=M} \sum_{i=1}^{i=N} |\phi^{n+1} - \phi^n|}{\sum_{j=1}^{j=M} \sum_{i=1}^{i=N} |\phi^{n+1}|} < 10^{-6} \quad (20)$$

where ε is the tolerance; M and N are the number of grid points in the x and y directions, respectively.

In order to ensure the grid-independence solutions, a series of trial calculation conducted for different grid size: 51x101, 101x201, 151x251 and 401x501. The results of the average Nusselt numbers using different grid arrangements are 5.06, 5.1575, 5.2565 and 5.2573. It observed that

difference between the result of the grid 151x251 and that of the grid 401x501 is less than 0.015%. Consequently, to optimize appropriate grid refinement with computational efficiency, the grid 151x251 is chosen for all computations.

5. Model Validation:

The accuracy of FVM and FORTRAN code was tested against the analytical solution for Poisuille-hartmann flow of a conducting and viscous fluid between two stationary plates with uniform external magnetic field orthogonally to the plates. Assuming the wall at $y=0$ and $y=H$ and that the fluid velocity on the walls is zero

and that the fluid moves in X direction under the influence of a constant pressure gradient, as shown in fig.5 illustrated the computed and analytical velocity profile. It is appears in a very good agreement

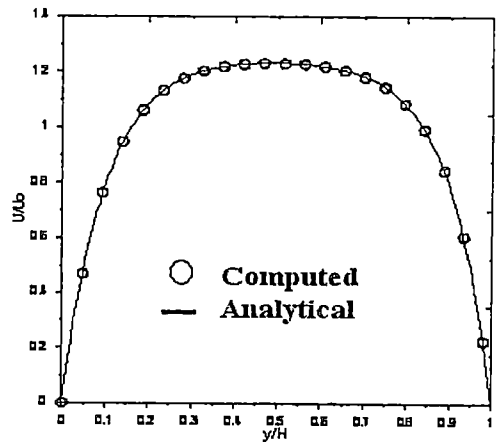


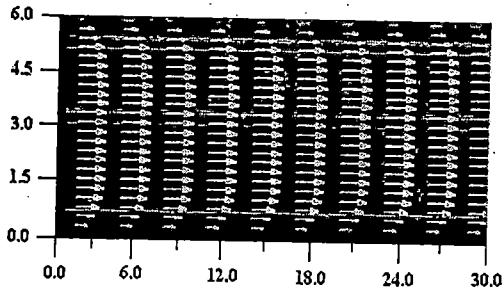
Fig.5 analytical and computed v. profile

The comparing between the flow fields obtained with PIV for the fully developed flow with and without the effect of the electromagnetic Lorentz body force, in the main plan, we note that the velocity has the maximum value in the most of the channel regions and the boundary layer is compressed due to the action of the Lorentz body force which creates a new boundary layer proportional with the inverse of the Hartmann's number. As

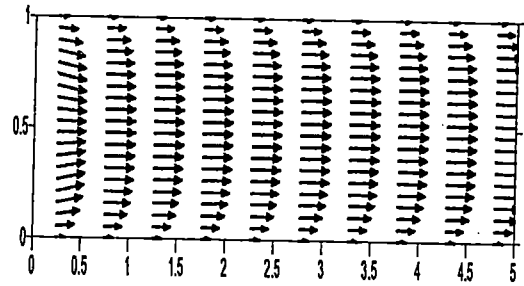
E. A. El-Agouz and M.I. Amro

shown in fig. 6(a-b), the accuracy of the numerical model also is verified by comparing the temperature contours of the present work and the temperature contours

calculated by Brian H. Dennis and George S. Dulikravich, 2001 [1] this could be founded in fig.8 (a-b) the comparison shown a good agreement

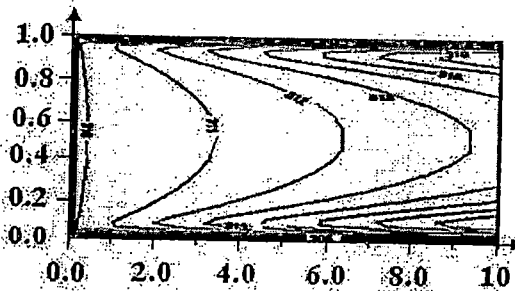


a. V-profile experimental (PIV), (L/H=5)

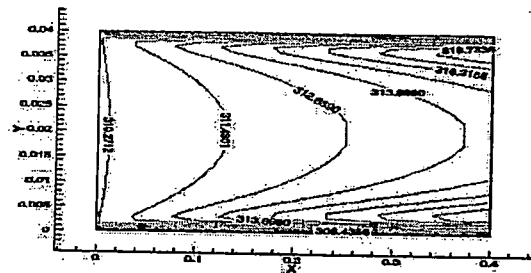


b. V-profile computed with code

Fig.6 comparison between (PIV) measured and computed velocity profiles



a. Computed temperature contour, present work



b. Temperatures contours Brian et al. 2001 [1]

Fig.7 Comparison between temperature contours for present work (a) and Brian et al. 2001 [1], at (Gr/Re = 10, Ha = 1000)

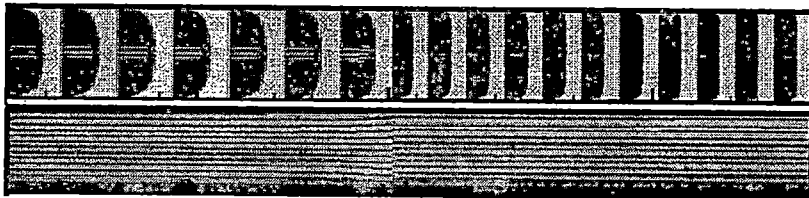
6. Results and discussion:

Fig.8 (a-b) illustrates PIV flow field in two measuring planes, first, the vertical or main plane in which the velocity distribution looks like the velocity exit from a honeycomb and the secondary plane which is known as M shape velocity profile appear due to the Lorentz force which decelerates

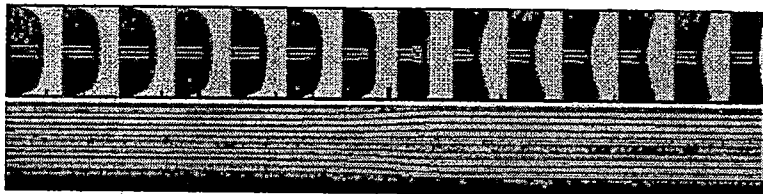
or accelerates the flow field depending on the values of external electric current factor. For the represented case, the flow field is measured with PIV laser system by applied magnetic field which creates an induced electric current, coupled with the applied magnetic field to create Lorentz body force. The creating force opposes

the flow direction and creating new features for flow field. These characteristics represent reduction of the boundary layer thickness in the main and side plane. The new boundary layer is smaller than the hydrodynamic fully developed case and proportional to the inverse of Hartmann number in main plane and with the inverse of the Hartmann

squire root in side plane. The electromagnetic force creating a high velocity gradient near the solid walls. This due to the combined effect of Lorentz force and the buoyancy force. Figs.8 (a & b) show also the fully developed velocity distributions before the main and side plane to appear the difference between the flow with and without electromagnetic forces.



a. PIV fully developed and main flow plane



b. PIV fully developed and side plane

Fig. 8 main plane (a) and side plane (b) with fully developed case before them measured by PIV

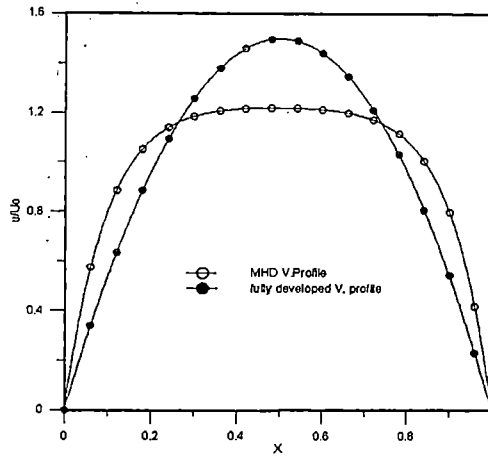


Fig.9 Computed fully developed flow with and without Lorentz force

Fig.9 represents comparison between the parabolic fully developed inlet velocity profile which has the maximum value 1.56 of the inlet average velocity. It shows that the profile under the induced electric field

(magnetic field) has a compacted boundary layer and the maximum velocity founded in most regions outside the boundary layers and its value depends upon the value of Hartmann number.

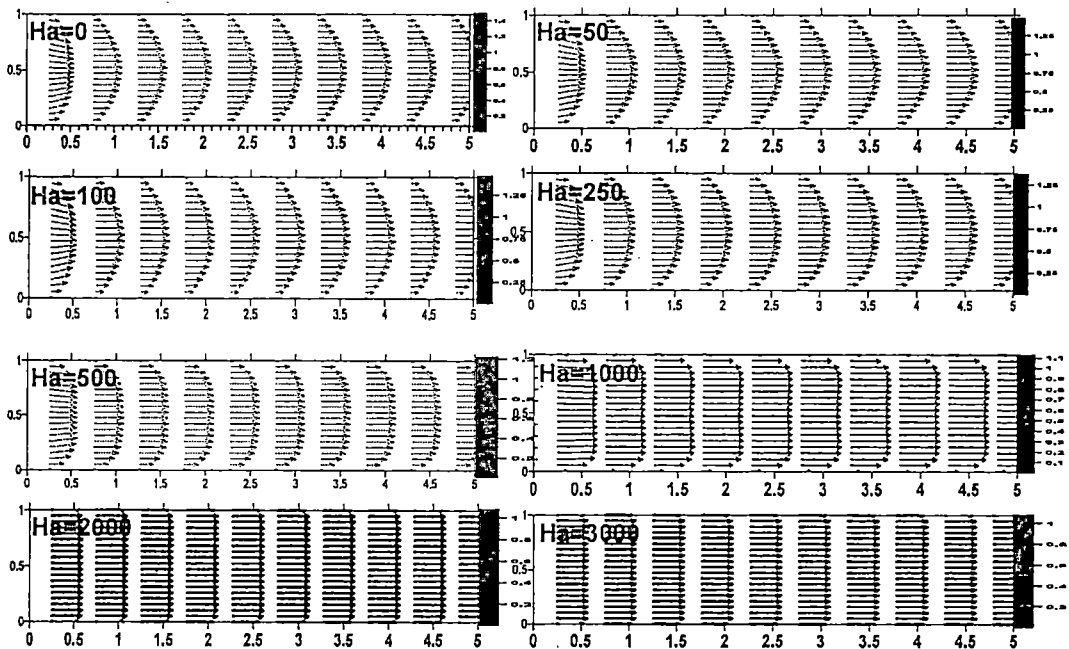


Fig.10 Computed vel., field $Re = 50$, $Ef = 0$, $Pr = 7$, $Gr = 1000$ at different Hartmann numbers

In Fig.10 the velocity fields were presented at constant Reynolds's number, $Re = 50$ for

different values of the Hartmann number from, 0 – 3000. It appears that the

maximum velocity values decrease as the Hartmann number increases. In addition, thickness decreases when Hartmann number increases and the profile is flat. These features are due to the higher values

for the Lorentz force and buoyancy force which create the high values of velocity gradient near the walls. These features increase as Hartmann number increases.

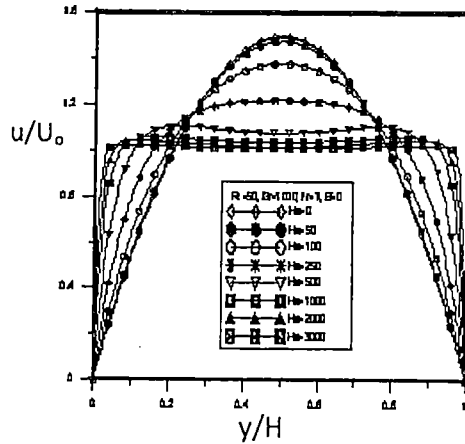


Fig. 11 Velocity profiles at $Re = 50$ and different values of Hartman number

In Fig.11 the velocity profiles shown for different Hartmann number. It shows that the maximum velocity decreases and the profile becomes more flatting as the Hartmann number increases. As the

Hartmann increases the boundary layer thickness decreases this decreases also the thermal boundary layer thickness and this enhancement the heat rates.

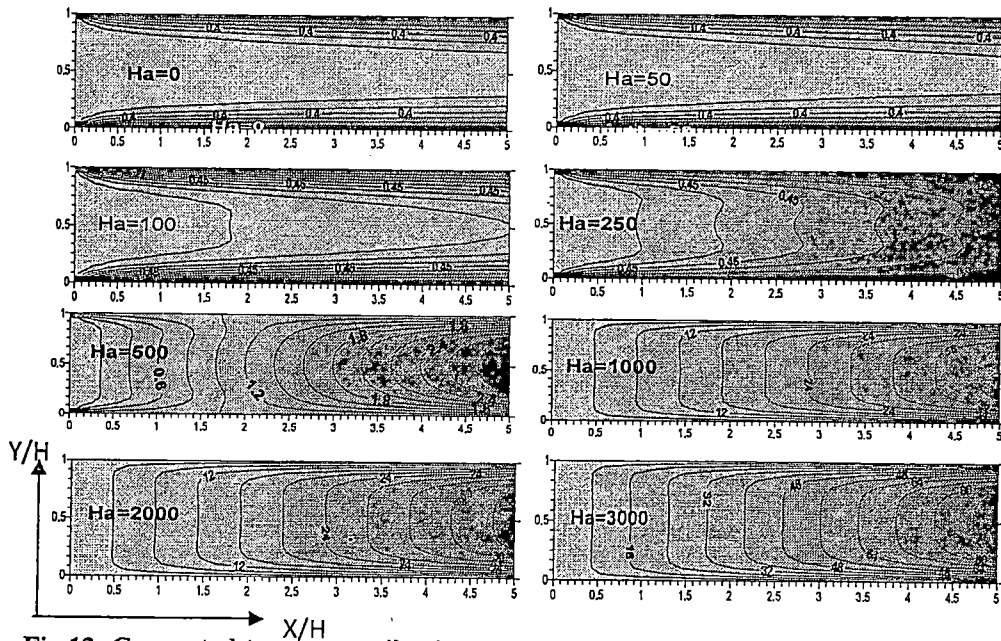


Fig.12, Computed temperature contributions for $Re = 50$, $Ef = 0$, $Pr = 7$, $Gr = 1000$ at different Hartmann numbers Ha

E. A. El-Agouz and M.I. Amro

Figure 12 represents the temperature contours at a constant Reynolds number ($Re = 50$) for different values for the Hartmann number ($Ha = 0 - 3000$). All temperatures contours in this case computed with no effect to the external electric field parameter ($Ef = 0$). Results showed that as the Hartmann number increases, the Lorentz force created by the coupling between the induced electric field and the applied magnetic field increases. This force action opposite the flow direction and alters the heat transfer characteristics, due to the decelerating of the flow velocity. A direct result for the increasing of the induced current is creating an internal heat flux in the flow so, the temperature distribution and temperature difference between the inlet temperature T_0 and the fluid temperature T at any position is larger than the difference between the inlet and wall temperature. Due to that, as the Hartmann's number, Ha increases the average Nusselt number, Nu decreases.

The relation between the Nusselt number Nu and the Hartmann number Ha depends on the value of external electric field parameter, when the effect of external electric field is taken into consideration.

When the value of external electric field parameter Ef is more than zero but less than unity, it is enhancement heat transfer

and average Nusselt number Nu increases as Ef increases. This is due to that the external electric field which decreases the Joule dissipating energy, this showed good in Fig.13 for temperature contours, one could notes that the temperature levels decreases as Ef increases.

Just the value of external electric field parameter Ef reaches unity, it is found that the electric fields do not have any effect on the flow since the effect of external electric field deleting the effect comes from the induced field so, at this value for Ef ; it is found that the Joule dissipating energy is vanished.

As electric field parameter values more than unity, the Joule dissipating energy increases and the average Nusselt number decreases and this alters the heat transfer. But as showed in Fig.13 although the Nusselt number decreases in this case but the high levels of temperature contours do not reach the channel walls and this protect the channel from overheating.

Figure 14 represents two velocity profile each at a Reynolds's number $Re = 50$ and Hartmann's number, $Ha = 1000$. The first at external electrical factor $Ef = zero$ while the second at $Ef = 6$. From the figures we get that the applied external electrical field has not a significant effect on the shape of the velocity distribution while its effect illustrated good in the temperature contour.

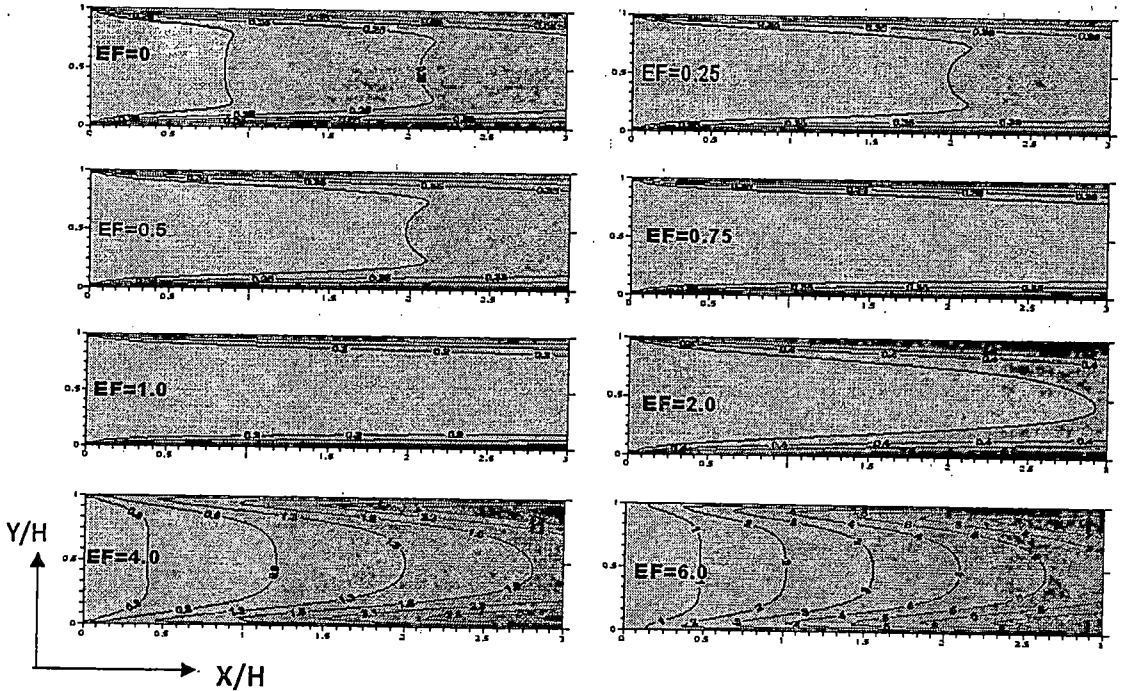


Fig.13, Computed temp., contours for $Re = 50$, $Gr = 1000$, $Pr = 7$, $Ha=1000$ at different External Electric field Parameter E_f

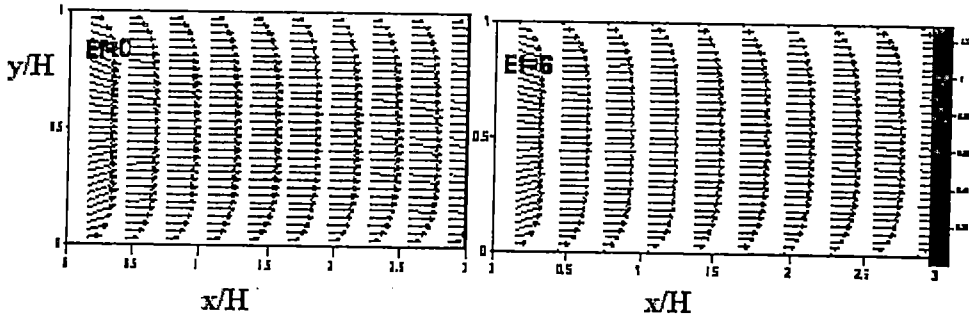


Fig.14 Computed velocity distributions for $Re = 50$, $Gr = 1000$, $Pr = 7$, $Ha = 1000$ for $E_f = (0 \& 6)$

6. Conclusions

The Electromagnetohydrodynamics mixed convection flow through rectangular channel is studied experimentally and solved numerically. The governing equations of the model consist of the mass, momentum and energy equations. The Vorticity-stream function formulation is

used and the finite volume technique is applied to discrete the model equations. The algebraic equations are solved by using the Gauss-elimination method.

Forced convection heat transfer to an EMHD fluid of a flat duct is investigated in the present work. Both Joule heating and viscous dissipation are taken into

E. A. El-Agouz and M.I. Amro

consideration. Influence of the Hartmann number, Reynolds number and external electric field parameter on temperature profile and local Nusselt number are discussed.

When the value of external electric field parameter is equal to zero, the rate of heat transfer is altering and average Nusselt number is decreasing with the increasing of the induced electric current.

In case of effect of the external electric current, the rate of heat transfer and flow velocities depend on the current value and direction. When E_f is negative, the current decreases the rate of heat transfer, and altering its characteristics, also lowering the flow velocities since the channel working as an electromagnetic generator.

When the external electric parameter P_{EM} equal to unity, the energy obtained from the applied external current is equal to the energy of flow and the channel is not affect with the electric field and the Joule dissipating energy is vanished. The channel is working as an electromagnetic flow meter.

The heat transfer rate and Nusselt number are largely effect and increase with increasing of the external electric field parameter up till a certain value less than unity depends on the Ha number effect. After this value, Joule dissipating energy is increasing and average Nu decreased.

When P_{EM} values increase over than unity, the channel is working as an electromagnetic accelerator.

The model is valid for any values of Prandtl, Eckert, and Grashof numbers. The comparisons between the measurements of the present work and other published results show good agreement.

REFERENCES

- [1] Brian H. Dennis and George Dulikravich "Electromagnetohydrodynamic (EMHD): Numerical Experiments in Steady Planar Flows" Copyright by ASME Journal, 2000 and AMD. Vol.244/MD-Vol.92, Recent Advanced in the Mechanics of Structured Continuo – 2000.
- [2] Setsuo Takezawa, Hiroshi Tamama, Kazumi Sugwawa, Hiroshi Sakai, Chiaki Matsuyama, Hiroak Morita, Hiromi Suzuki and Yoshihiro Ueyama " Operation of the Thruster for Superconducting Electromagnetohydrodynamics Propulsion Ship " YAMATO 1" Journal of the MESJ , Vol.29, No.6, March , 1995.
- [3] Sergei I. Sidorenkov, Thanh Q. Hua and Hideo Araseki "Magnetohydrodynamics and Heat Transfer Benchmark Problems for Liquid-Metal Flow in Rectangular Ducts" Journal of Fusion Engineering and Design 27 (1995) 711-718.

- [4] Hiroshige Kumamaru, Satoshi Kodama, Hiroshi Hirano and Kazuhiro Itoh " three- dimensional numerical calculations on liquid metal magnetohydrodynamic flow in Magnetic field Inlet region" Journal of Nuclear Science and technology, Vol. 41, No. 5, pp. 624-631, May 2004.
- [5] J. Mao, S. Aleksandrova, S. Molokov "Joule Heating in Magnetohydrodynamic Flows in Channels with Thin Conducting Walls" International Journal of Heat and Mass Transfer 51 (2008) 4392-4399.
- [6] P.R. Sharma and G. Singh "Numerical Solution of Transient MHD Free Convection Flow of an Incompressible Viscous Fluid along an Inclined Plate with Ohmic Dissipation "International Journal of Applied Mathematics and Mechanics 5 (5): 57-65, 2009.
- [7] N. Vetcha, S. Smolentsev and Mohamed Abdou "Theoretical Study of Mixed Convection in Poloidal Flows of DCLL Blanket" Journal of Fusion Science and Technology, vol. 56, Aug. 2009.
- [8] N. Aslan "An Incompressible Magnetohydrodynamics Solver" Journal of Theoretical and Applied Physics, 3-4, 1-9, 2010.
- [9] H. Saleh and I. Hashim, "Flow Reversal of Developed Mixed Convection in Vertical Channels" China Journal of LETT. Vol.27, No.2, 2010, 024401.
- [10] J.C. Umavathi, I.C. Liu and Prathap Kumar "Fully Developed Magneto Convection Flow in a Vertical Rectangular Duct" Journal of Heat and Mass Transfer, Vol. 47:1-11, 2011.
- [11] Peter L. O'Sullivan and Sedat Biringen "Direct numerical Simulation of Low Reynolds Number Turbulent Channel flow With EMHD Control "The work is supported by the office of Naval Research under grant number DOD N00014-95-1-0419, 1997. Computations were performed on a Cray C916 at the US Army Corps of engineers. Experiment Station Water-ways.
- [12] Eugenio Schuster and Lixiang Luo," Mixing Enhancement in 2D Magnetohydrodynamic Channel Flow by Extremum Seeking Boundary Control" American Control Conference, Hyatt Regency Riverfront. St. Louis, MO. USA, June 10-12, 2009.
- [13] S. Ganesh and S. Krishnambal "Magnetohydrodynamic Flow of Viscous Fluid between Two Parallel Porous Plates" Journal of Applied Sciences 6 (11): 2420-2425, 2006.
- [14] T. Linga Raju and P.S. R. Murty " MHD Heat Transfer Aspects Between Two Parallel conducting Porous Walls in a Rotating System, with Hall Currents"

A. M. El-Zahaby, M.K. Bassiouny, A. Khalil, E.A. El-Shenawy,

E. A. El-Agouz and M.I. Amro

African Journal of Mathematics and
Computer Science Research Vol. 4 (7), pp.
242-250 July, 2011.

[15] M.M. Rahman, S. Parvin, R. Saidur
and N.A. Rahim " Magnetohydrodynamic
Mixed Convection in a Horizontal Channel
with an Open Cavity" Journal of
International Communications in Heat and
Mass Transfer 38 (2011), 184-193.

[16] Raffel, M., Willert c. and
Kompenhans, J. "Particle Image
Velocimetry, a Particle Guide" Springer
Verlag, 1998.

[17] Hartmann, J., " Hg-Dynamics I
"Theory of laminar Flow of an Electrically
Conductive Liquid in a Homogenous
Magnetic Fields" Dansk Videnskab, Mat.-
Fys. Medd., Vol. 15, No.6, 1937.

[18] Hartmann, J., and Lazarus, F., "Hg-
Dynamics II: Experimental Investigations
on the Flow of Mercury in a Homogenous
Magnetic Field," Dansk Videnskab, Mat.-
Fys. Medd., Vol. 15, No.7, 1937.

[19] Patanker, S. V., "Numerical Heat
Transfer and Fluid Flow" Hemisphere
publishing company, New York, 1980.

[20] Versteeg, H. K. and Malalasekera, W.
" An Introduction to Computational Fluid
Dynamics the Finite Volume Method",
Longman Malaysia, TCP, 1995.